PASJ: Publ. Astron. Soc. Japan **63**, S531–S536, 2011 March 25

A Possible Tilted Orbit of the Super-Neptune HAT-P-11b*

Teruyuki HIRANO,[1,2] Norio NARITA,[3] Avi SHPORER,[4,5] Bun'ei SATO,[6]
Wako AOKI,[3] and Motohide TAMURA[3]
[1] *Department of Physics, The University of Tokyo, 7-3-1 Hongo, Bonkyo-ku, Tokyo 113-0033*
hirano@utap.phys.s.u-tokyo.ac.jp
[2] *Department of Physics, and Kavli Institute for Astrophysics and Space Research, Massachusetts Institute of Technology, Cambridge, MA 02139, USA*
[3] *National Astronomical Observatory of Japan, 2-21-1 Osawa, Mitaka, Tokyo 181-8588*
[4] *Department of Physics, Broida Hall, University of California, Santa Barbara, CA 93106, USA*
[5] *Las Cumbres Observatory Global Telescope Network, 6740 Cortona Drive, Suite 102, Santa Barbara, CA 93117, USA*
[6] *Department of Earth and Planetary Sciences, Tokyo Institute of Technology, 2-12-1 Ookayama, Meguro-ku, Tokyo 152-8551*

(Received 2010 September 6; accepted 2010 November 15)

Abstract

We report on the detection of the Rossiter–McLaughlin effect for the eccentric, super-Neptune exoplanet HAT-P-11b, based on radial-velocity measurements taken with the High Dispersion Spectrograph mounted on the Subaru 8.2 m telescope, and simultaneous photometry with the LCOGT 2.0 m Faulkes Telescope North, both located in Hawaii. The observed radial velocities during a planetary transit of HAT-P-11b show a persistent blue-shift, suggesting a spin–orbit misalignment in the system. The best-fit value for the projected spin–orbit misalignment angle is $\lambda = 103^{\circ}{}^{+22^{\circ}}_{-18^{\circ}}$. This fact suggests that not only hot-Jupiters, but also super-Neptunes like HAT-P-11b had once experienced dynamical processes, such as planet–planet scattering or Kozai migration.

Key words: stars: planetary systems: individual (HAT-P-11) — stars: rotation — techniques: photometric — techniques: radial velocities — techniques: spectroscopic

1. Introduction

Transiting exoplanetary systems provide a unique probe to investigate the dynamical history of planetary systems discovered today. The Rossiter–McLaughlin effect (hereafter, the RM effect), which was originally discussed for stellar eclipsing binaries (Rossiter 1924; McLaughlin 1924), is an apparent radial-velocity (hereafter, RV) anomaly during a planetary transit caused by partial occultation of the rotating stellar surface (e.g., Queloz et al. 2000; Winn et al. 2005; Ohta et al. 2005; Gaudi & Winn 2007). Through the RM effect, one can estimate the angle between the stellar rotation axis and the planetary orbital axis projected onto the sky plane. This angle, which we denote by λ, is strongly related to the formation and migration history of close-in exoplanets.

The standard formation theory of close-in gas-giants (hot-Jupiters) suggests that they formed outside the so called snow-line, which is usually located at a few AU away from the host star, and then migrated inward due to some migration process (e.g., Lin et al. 1996; Chambers 2009; Lubow & Ida 2010). While migration processes, such as disk–planet interactions (type I or II migration), predict relatively small values of λ, dynamical processes including planet–planet scattering and Kozai cycles might produce a large value of λ (e.g., Wu et al. 2007; Fabrycky & Tremaine 2007; Nagasawa et al. 2008; Chatterjee et al. 2008). The observed distribution of λ and its host star dependence would help reveal the dynamical history of exoplanetary systems.

To this point, the RM effect has been measured for approximately 30 transiting hot-Jupiters (see table 1 of Winn et al. 2010a). The observational results indicate that the spin–orbit axes in some of the systems are well-aligned at least when projected on the plane of the sky, but others show significant misalignment. Eccentric exoplanetary systems, where $e \gtrsim 0.1$, and systems whose central stars are massive ($M_{\star} \gtrsim 1.2\,M_{\odot}$) are more likely to show strong misalignment (Winn et al. 2010a). Specifically, out of the thirteen eccentric transiting systems (CoRoT-9, CoRoT-10, GJ 436, HAT-P-2, HAT-P-11, HAT-P-14, HAT-P-15, HD 17156, HD 80606, WASP-8, WASP-14, WASP-17, and XO-3), the RM effect has been observed for seven systems (HAT-P-2, HD 17156, HD 80606, WASP-8, WASP-14, WASP-17, and XO-3). Among them, five systems have been reported to have significant spin–orbit misalignment (HD 80606, WASP-8, WASP-14, WASP-17, and XO-3) based on measurements of the RM effect (Hébrard et al. 2008; Winn et al. 2009b; Queloz et al. 2010; Winn et al. 2009a; Triaud et al. 2010). In addition, Schlaufman (2010) reported the possibility of a spin–orbit "misalignment along the line-of-sight" in other eccentric systems (e.g., HD 17156 and HAT-P-14) based on an analysis of stellar rotational periods (note that the sky-projected spin–orbit alignment angle for HD 17156 has been reported to be $\lambda = 10.^{\circ}0 \pm 5.^{\circ}1$ by Narita et al. 2009a).

In this paper, we focus on the RM effect of the super-Neptune HAT-P-11b. So far, the RM effect has been observed only for hot-Jupiters. In order to obtain a clearer insight into planetary migration processes, we need to measure the RM effect for a wider range of planetary and stellar parameters.

* Based on data collected at Subaru Telescope, which is operated by the National Astronomical Observatory of Japan.

The transiting super-Neptune exoplanet HAT-P-11b (Bakos et al. 2010) was detected by the HATNet transit survey (Bakos et al. 2004) and confirmed by subsequent RV measurements at Keck with HIRES. HAT-P-11b orbits a bright K dwarf star ($V \sim 9.6$ mag) with an orbital period of ~ 4.9 days. Its planetary radius, $R_{\rm p} = 0.422 \pm 0.014\,R_{\rm J}$, is one of the smallest among the known transiting exoplanets. Although HAT-P-11b is a difficult target for an RM measurement due to its small size, the detection of the RM effect for Neptune-sized planets are of great importance for making further progress in studying migration histories.

The remainder of the present paper is organized as follows. In section 2 we report on new spectroscopic and photometric observations of the HAT-P-11 system using the High Dispersion Spectrograph (HDS) installed on the 8.2 m Subaru Telescope, and the LCOGT 2.0 m Faulkes Telescope North (FTN). The new observations include simultaneous transit spectroscopy and photometry of HAT-P-11b on 2010 May 27 UT as well as several out-transit RV datasets to determine the orbital (Keplerian) motion of HAT-P-11. Data analysis is presented in section 3. We combine the new photometric and RV dataset with the published RV data by Bakos et al. (2010) and simultaneously determine the orbital and RM parameters in section 4. We report that the RV anomaly during the transit shows a possible spin–orbit misalignment in the system. Finally, section 5 summarizes our findings.

2. Observations

2.1. Subaru Spectroscopy

We conducted spectroscopic observations of HAT-P-11 with Subaru/HDS on 2010 May 21, 27, and July 1 UT. We employed the Std-I2b setup on May 21 and 27, and the Std-I2a setup on July 1. Due to bad seeing during the May observations, we needed to broaden the slit width, which we set to $0\farcs8$, yielding a spectral resolution of $R \sim 45000$. We set it to $0\farcs4$ for the July observation, corresponding to $R \sim 90000$. We observed the target with the Iodine cell for a precise wavelength calibration. Adopting exposure times of 360–420 seconds, we obtained a typical signal-to-noise ratio (S/N) of 150–200 per pixel after extracting the one-dimensional spectra.

We reduced the raw data with the standard IRAF procedures (using the echell package), and extracted one-dimensional spectra. We then input the spectra into the RV analysis routine. The RV analysis for Subaru/HDS is described in detail by Sato et al. (2002) and Narita et al. (2007). Specifically, in order to obtain the stellar template spectrum, we adopted a method developed by Butler et al. (1996), which uses a high S/N, high-resolution observed spectrum of the host star without the Iodine cell. We took that stellar template spectrum during the July 1 observation, and deconvolved it with the instrumental profiles, which were estimated by the rapid rotator plus I_2 spectrum. The output relative RVs are summarized in table 1. The reported errors based on the RV analysis do not include stellar "jitter", which has been reported to be significant for HAT-P-11. The measured RVs as well as the published Keck data by Bakos et al. (2010) are plotted in figure 1.

Table 1. Radial velocities measured with Subaru/HDS.

Time [BJD (TDB)]	Relative RV [m s^{-1}]	Error [m s^{-1}]
2455338.06233	21.81	3.50
2455338.06784	25.54	3.17
2455343.88397	2.48	2.61
2455343.89499	4.69	2.27
2455343.90050	−0.64	2.53
2455343.90601	8.59	2.73
2455343.91152	−1.56	2.52
2455343.91703	−3.65	2.24
2455343.92254	3.52	2.46
2455343.92805	−1.20	2.45
2455343.93356	−4.11	2.20
2455343.93907	−0.79	2.55
2455343.94459	−2.32	2.27
2455343.95010	−2.89	2.29
2455343.95562	−0.98	2.50
2455343.96114	−0.79	2.48
2455343.96666	−1.78	2.60
2455343.97217	0.94	2.67
2455343.97769	1.69	2.29
2455343.98321	1.83	2.58
2455343.98873	1.82	2.48
2455343.99425	−2.05	2.43
2455343.99976	4.62	2.02
2455344.00528	0.70	2.80
2455344.01080	−4.27	2.72
2455344.01631	−4.03	2.62
2455344.02183	−5.10	2.32
2455344.02734	0.28	2.76
2455378.96562	−11.69	3.45
2455378.97044	−8.31	3.74
2455378.97543	−8.92	3.75
2455378.98025	−3.12	3.54
2455378.98507	−4.25	3.76
2455379.09708	−5.42	3.77
2455379.10189	−4.86	3.62
2455379.10674	−4.84	3.73
2455379.11156	2.36	4.05
2455379.11639	−6.53	3.29
2455379.12123	−5.33	3.93
2455379.12605	1.63	3.55

2.2. Simultaneous FTN Photometry

In order to derive an accurate estimate of the start and end times of the transit, we obtained a photometric light curve of the same transit event on 2010 May 27 UT. We observed with FTN and the Spectral Instruments camera with the Pan-STARRS-Z filter. The camera has a back-illuminated Fairchild Imaging CCD, and we used the default 2×2 pixels binning mode, with an effective pixel scale of $0\farcs304$ pixel^{-1}. The telescope was defocused and the $10\farcs5 \times 10\farcs5$ field of view (FOV) was positioned so that the guiding camera FOV would contain a suitable guide star. We used an exposure time of 10 seconds, and the median cycle time was 30.6 seconds. FTN observations started at 2010 May 27 09:08 UT and ended

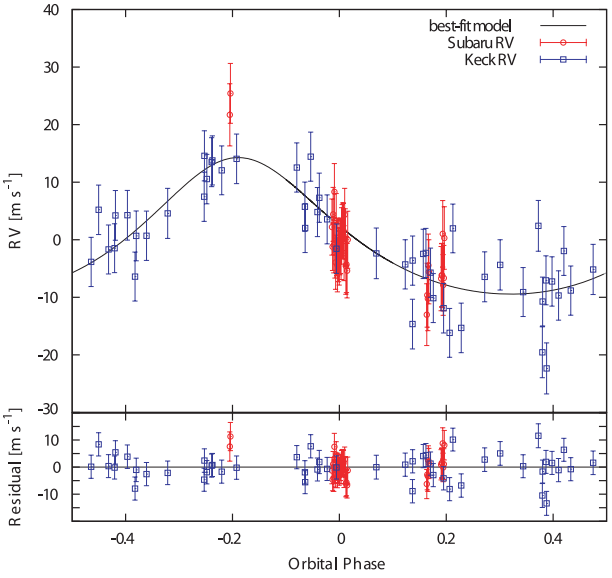

Fig. 1. RVs taken by the Subaru/HDS (red) and the published ones taken with Keck/HIRES (blue). The best-fit curve is shown in the solid (black) line. Each RV error shown in this figure includes stellar jitter. The RV residuals from the best-fit curve are shown in the bottom panel.

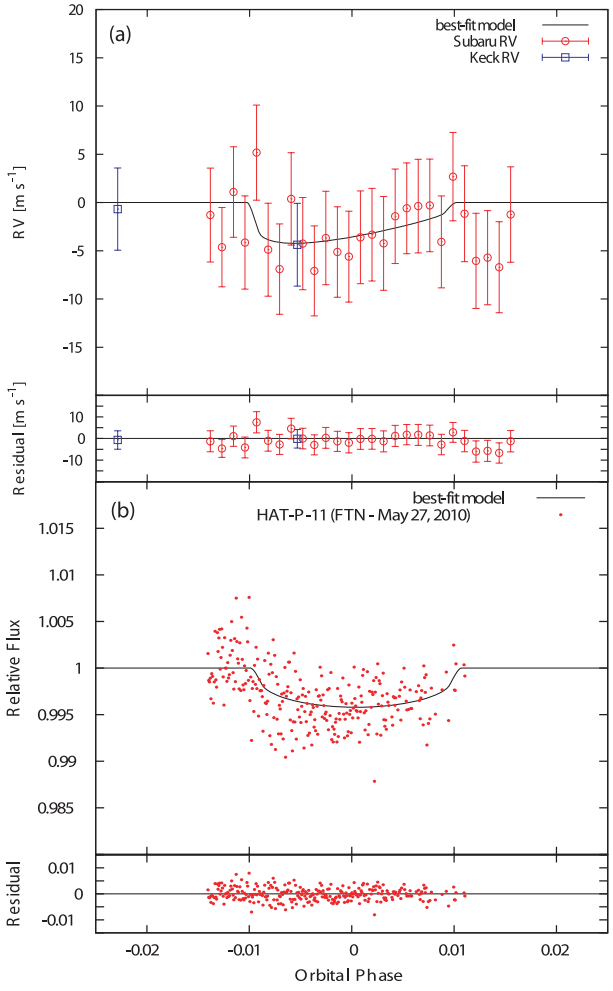

Fig. 2. (a) Same as figure 1, but zoomed around the transit after subtracting the orbital motion (the Keplerian plus constant long-term drift). (b) Simultaneous photometry of HAT-P-11 and their residuals from the best-fit light curve, obtained on 2010 May 27 UT with FTN and the Pan-STARRS-Z filter. The best-fit value for the transit center is $2455343.95052^{+0.00153}_{-0.00237}$ [BJD (TDB)]. Note that we have less photometric data around the transit-end due to bad weather conditions.

at 2010 May 27 13:09 UT, an overall duration of 4.0 hours. Photometry was done with aperture photometry, and the light curve was calibrated using several non-variable stars in the field. The observing conditions deteriorated at FTN during the HAT-P-11 transit observation, and only a small number of sufficient quality exposures were obtained during egress. The dome had to be closed soon after the transit ended. The resultant photometric light curve is shown in figure 2 (panel b).

3. Analysis

In order to estimate the spin–orbit misalignment angle, λ, from the observed RV anomaly during the transit, we need an explicit relation between the position of the planet on the stellar disk and the RV anomaly. Following the procedure described by Winn et al. (2005) and Hirano et al. (2010), we performed the following mock data simulation. First, we broadened a theoretically synthesized spectrum for the same stellar type as HAT-P-11 (the effective temperature equal to 4750 K) so that the broadened spectral lines would have a rotational velocity of $v \sin i_{\rm s} = 1.5\,{\rm km\,s^{-1}}$. Second, we had the original unbroadened spectrum scaled (multiplied) by f and Doppler-shifted by $v_{\rm p}$, where f and $v_{\rm p}$ are the ratio of the flux from the occulted portion on the stellar surface to the disk-integrated flux and the line-of-sight component of the rotational velocity of the occulted stellar portion, respectively. Thus, this scaled (and Doppler-shifted) spectrum corresponds to the spectral contribution of the portion on the stellar disk blocked by the planet. We then subtracted the scaled spectrum from the one broadened by the first step, thus obtaining the mock spectrum during a transit. Changing the relative decrease in flux f and the velocity component $v_{\rm p}$, we generated many simulated spectra during a transit, and put them into the RV analysis procedure, as we did for the observed spectra. After fitting the output velocity anomaly, Δv, with the input parameters f and $v_{\rm p}$, we derived the following empirical relation:

$$\Delta v = -f v_{\rm p}\left[1.16 - 0.205\left(\frac{v_{\rm p}}{v \sin i_{\rm s}}\right)^2\right], \quad (1)$$

where $v \sin i_{\rm s}$ is the projected stellar rotational velocity of HAT-P-11, which we set here as $v \sin i_{\rm s} = 1.5\,{\rm km\,s^{-1}}$ based on the analysis of stellar obsorption lines (Bakos et al. 2010).

Bakos et al. (2010) reported that the HAT-P-11 system shows a long-term RV drift over one-year of observations of the system. Since our new observations span only about one month, we could not determine the long-term RV drift from our new Subaru dataset alone. Instead, we assumed the RV drift as to be $\dot{\gamma} = 0.0297 \pm 0.0050\,{\rm m\,s^{-1}\,d^{-1}}$, as reported by Bakos et al. (2010).

Our single transit light curve can not significantly refine the light-curve parameters determined by Bakos et al. (2010), based on several transit light curves. We thus fixed the system parameters of Bakos et al. (2010) for the orbital period, $P = 4.8878162 \pm 0.0000071$ d, and the orbital inclination, $i_{\rm o} = 88.^{\circ}5 \pm 0.^{\circ}6$. We fixed these parameters at the central value, and use the light curve model by Ohta et al. (2009). Assuming a quadratic limb-darkening law, we fixed the limb-darkening coefficients for the transit light curve as $u_1 = 0.35$ and $u_2 = 0.26$ (Claret 2004). Instead of fixing the semi-major axis scaled by the stellar radius, $a/R_{\rm s}$, and the radius ratio, $R_{\rm p}/R_{\rm s}$, we let these be free, but put a priori constraints on these parameters based on the published values. The remaining free parameters, except for $a/R_{\rm s}$ and $R_{\rm p}/R_{\rm s}$, are as follows: the midtransit time, $T_{\rm C}$ determined by simultaneous photometry, the RV semi-amplitude, K, the orbital eccentricity, e, the argument of periastron, ω, the spin–orbit misalignment angle, λ, the projected stellar rotational velocity, $v \sin i_{\rm s}$, and the RV offset between the Subaru and Keck datasets. The χ^2 statistic in this case is expressed as:

$$\chi^2 = \sum_i \left[\frac{v^{(1)}_{i,\rm obs} - v^{(1)}_{i,\rm model}}{\sigma^{(1)}_i} \right]^2 + \sum_j \left[\frac{v^{(2)}_{j,\rm obs} - v^{(2)}_{j,\rm model}}{\sigma^{(2)}_j} \right]^2 + \left[\frac{R_{\rm p}/R_{\rm s} - 0.0576}{0.0009} \right]^2 + \left[\frac{a/R_{\rm s} - 15.58}{0.50} \right]^2, \quad (2)$$

where $v^{(1)}_{i,\rm obs}$ and $v^{(1)}_{i,\rm model}$ are the RV values, and $v^{(2)}_{j,\rm obs}$ and $v^{(2)}_{j,\rm model}$ are the relative flux values, obtained by the observations and model calculations, respectively. The RV and flux errors are represented by $\sigma^{(1)}_i$ and $\sigma^{(2)}_j$, respectively. Note that we adopted a "stellar jitter" of $\sigma_{\rm jitter} = 4.1\,{\rm m\,s^{-1}}$ so that the resultant reduced χ^2 for the observed RVs would become unity, and computed modified RV errors, $\sigma^{(1)}_i$, by

$$\sigma^{(1)}_i = \sqrt{\sigma^2_{0,i} + \sigma^2_{\rm jitter}}, \quad (3)$$

where $\sigma_{0,i}$ are the reported errors by the RV analysis. We used the modified RV errors $\sigma^{(1)}_i$ for estimating the errors of the free parameters.

4. Results and Discussion

We determined the model parameters so that the χ^2 statistic would take its minimum value by the AMOEBA algorithm (see Narita et al. 2008, 2010). Figure 1 presents the phase-folded RVs obtained by Subaru and Keck, along with the best-fit RV curve. In this figure, we have subtracted the long-term RV variation, $\dot{\gamma}$, from the observed values. In figure 2, we also show the RVs around the transit (phase ~ 0), as well as the simultaneous photometry with FTN. The observed RVs show a persistent blue-shift throughout the transit, suggesting a spin–orbit misalignment. The best-fit values for the six parameters are summarized in table 2. The $1\,\sigma$ uncertainty for each parameter is estimated by the criterion $\Delta\chi^2 = 1.0$. The spin–orbit misalignment angle, λ, was estimated to be $\lambda = 103^{\circ}{}^{+22^{\circ}}_{-18^{\circ}}$. Since the Keck RV dataset covers most of the orbital phase outside of the transit, the estimated values for K, e, and ω are in good agreement with the reported values by Bakos et al. (2010).

Table 2. Best-fit parameters.

Parameter	Best-fit value
$T_{\rm C}$ [BJD (TDB)]	$2455343.95052^{+0.00157}_{-0.00237}$
K [m s^{-1}]	11.9 ± 0.9
e	0.204 ± 0.036
ω [°]	356^{+15}_{-13}
λ [°]	103^{+22}_{-18}
$v \sin i_{\rm s}$ [km s^{-1}]	$2.09^{+1.05}_{-0.96}$
$R_{\rm p}/R_{\rm s}$	0.0586 ± 0.0008
$a/R_{\rm s}$	$15.28^{+0.46}_{-0.43}$

The estimated stellar rotational velocity, $v \sin i_{\rm s} = 2.09^{+0.96}_{-1.05}\,{\rm km\,s^{-1}}$, by our RM analysis agrees with the spectroscopically measured value within $1\,\sigma$. In order to confirm the robustness of the estimated spin–orbit misalignment angle, λ, we tested the following two cases. First, instead of letting $v \sin i_{\rm s}$ be a free parameter, we fixed it as $v \sin i_{\rm s} = 1.5\,{\rm km\,s^{-1}}$ (the spectroscopically measured value), and fit the other five parameters. As a result, we obtained $\lambda = 106^{\circ}{}^{+24^{\circ}}_{-23^{\circ}}$, in good agreement with the main result described above. Second, we fixed the planet to the star radius ratio to the value determined by Dittmann et al. (2009), of $R_{\rm p}/R_{\rm s} = 0.0621 \pm 0.0011$, based on a photometric follow-up observation of the system. By adopting their results we obtained $\lambda = 104^{\circ}{}^{+21^{\circ}}_{-17^{\circ}}$, which is also consistent with the main result within 1σ. As expected in this case, we obtained a slightly smaller rotational velocity ($v \sin i_{\rm s} = 1.91^{+0.87}_{-0.86}\,{\rm km\,s^{-1}}$) than the main result. In both cases mentioned above, we found no significant difference in the other fitted parameters (K, e, ω) from the main result.

The spin–orbit misalignment angle, λ, is very sensitive to the RVs taken out-of-transit, which determine the Keplerian motion of HAT-P-11b. Our new dataset contains two, nine, and twelve out-of-transit RVs taken on 2010 May 21, 27, and July 1 UT, respectively. However, the number of RVs might not be sufficient in systems as HAT-P-11, where the planet is small and its host star is active. In addition, since the observations in May and July are separated by roughly one month, the long-term RV drift reported by Bakos et al. (2010) might have affected the result. If the long-term RV drift is actually caused by a secondary planet lurking in the HAT-P-11 system, the RV drift should modulate with time. In order to test the effect of a RV drift variation, we artificially changed the RV drift from $\dot{\gamma} = 0.0297\,{\rm m\,s^{-1}\,d^{-1}}$ into values shifted by $\pm 5\,\sigma$ (i.e., $\dot{\gamma} = 0.0547\,{\rm m\,s^{-1}\,d^{-1}}$ and $\dot{\gamma} = 0.0047\,{\rm m\,s^{-1}\,d^{-1}}$). This treatment only slightly changed the best-fit value for the spin–orbit misalignment angle ($\lambda = 105^{\circ}{}^{+24^{\circ}}_{-19^{\circ}}$ and $\lambda = 102^{\circ}{}^{+20^{\circ}}_{-17^{\circ}}$ for $\dot{\gamma} = 0.0547\,{\rm m\,s^{-1}\,d^{-1}}$ and $\dot{\gamma} = 0.0047\,{\rm m\,s^{-1}\,d^{-1}}$, respectively), both of which are consistent with the main result given in table 2. The long-term RV drift has less impact on estimating λ.

Although the measurement of the RM effect in the HAT-P-11 system seems to be challenging, due to the small size of the

planet and large stellar jitter, our result suggests a significant spin–orbit misalignment of the system. As we have described in section 1, five out of the seven eccentric hot-Jupiters where the RM effect has been observed have significant spin–orbit misalignment. Our result suggests that the super-Neptune HAT-P-11b migrated to its present location by dynamical scattering, or a long-term perturbation by an outer body, similarly to other eccentric hot-Jupiters. In contrast, the fraction of misaligned systems with circular orbits is significantly smaller (e.g., CoRoT-1, HAT-P-7, WASP-15; Pont et al. 2010; Narita et al. 2009b; Winn et al. 2009b; Triaud et al. 2010).

Winn et al. (2010a) suggested the interesting possibility that hot-Jupiters have a large initial spin–orbit misalignment caused by dynamical processes, but the host stars' obliquity could *decline* due to tidal interactions between hot-Jupiters and the stellar convective zone. Since convective zones are particularly well-developed in cooler and less-massive stars, we are likely to observe spin–orbit alignment around cool host stars. Although HAT-P-11 is a very cool star ($T_{\rm eff} = 4780 \pm 50$ K), this hypothesis also claims that the decay timescale of host star's obliquity is larger when the planet has a lower mass and a distant orbit from the host star [see equation (2) of Winn et al. 2010a]. According to their criteria, the HAT-P-11 system can show a spin–orbit misalignment, mainly because of the lower mass of HAT-P-11b. Moreover, as Matsumura et al. (2010) reported recently, since the tidal interaction between the planet and the host star is supposed to be small, the observed tilted orbit of HAT-P-11 b is likely to be primordial, which implies a dynamical origin, like planet–planet scattering in the system.

A comparison of the spin–orbit misalignment angle for HAT-P-11b with those of other transiting hot-Neptunes (e.g., GJ 436b and Kepler-4b) is quite interesting, because their host stars are of different spectral types (Kepler-4 is a G0 star and GJ 436 is an M2.5 star), while HAT-P-11b, GJ 436b, and Kepler-4b have similar planetary radii and masses (e.g., Butler et al. 2004; Shporer et al. 2009; Borucki et al. 2010). Further observational investigations concerning the formation and migration history of hot-Neptunes will be an interesting topic in the next decade.

5. Summary

We have measured the RM effect for one of the smallest transiting exoplanets known to date, HAT-P-11b. The exoplanet has a significant eccentricity, and is an interesting target for the RM effect. The observed RV anomaly during the transit suggests a significant spin–orbit misalignment of the system, of $\lambda = 103^{\circ}{}^{+22^{\circ}}_{-18^{\circ}}$. To confirm the spin–orbit misalignment decisively, however, it is necessary to measure even more RVs of the system during and outside transits, as well as to better characterize the long-term RV variation. Although challenging, the measurement of the RM effect for Neptune-sized exoplanets will extend the parameter space where planetary formation and migration theories will be studied in the near future.

Note added in proof (2010 November 26):

Winn et al. (2010b) independently measured the RM effect for HAT-P-11 and obtained a spin–orbit misalignment angle of $\lambda = 103^{\circ}{}^{+26^{\circ}}_{-10^{\circ}}$, based on observations with Keck/HIRES.

We are very grateful to Joshua N. Winn and Atsushi Taruya for helpful comments on our results. This paper is based on data collected at Subaru Telescope, which is operated by the National Astronomical Observatory of Japan. We acknowledge support for our Subaru HDS observations by Akito Tajitsu, a support scientist for the Subaru HDS. This paper also uses observations obtained with facilities of the Las Cumbres Observatory Global Telescope. The data analysis was in part carried out on a common-use data analysis computer system at the Astronomy Data Center, ADC, of the National Astronomical Observatory of Japan. T.H. and N.N. are supported by Japan Society for Promotion of Science (JSPS) Fellowship for Research (DC1: 22-5935, PD: 20-8141). M.T. is supported by the Ministry of Education, Sports, Culture, Science and Technology, Grant-in-Aid for Specially Promoted Research, 22000005. We wish to acknowledge the very significant cultural role and reverence that the summit of Mauna Kea has always had within the indigenous people in Hawaii.

References

Bakos, G., Noyes, R. W., Kovács, G., Stanek, K. Z., Sasselov, D. D., & Domsa, I. 2004, PASP, 116, 266
Bakos, G. Á., et al. 2010, ApJ, 710, 1724
Borucki, W. J., et al. 2010, ApJ, 713, L126
Butler, R. P., Marcy, G. W., Williams, E., McCarthy, C., Dosanjh, P., & Vogt, S. S. 1996, PASP, 108, 500
Butler, R. P., Vogt, S. S., Marcy, G. W., Fischer, A. A., Wright, J. T., Henry, G. W., Laughlin, G., & Lissauer, J. J. 2004, ApJ, 617, 580
Chambers, J. E. 2009, Ann. Rev. Earth, Planet. Sci., 37, 321
Chatterjee, S., Ford, E. B., Matsumura, S., & Rasio, F. A. 2008, ApJ, 686, 580
Claret A. 2004, A&A, 428, 1001
Dittmann, J. A., Close, L. M., Green, E. M., Scuderi, L. J., & Males, J. R. 2009, ApJ, 699, L48
Fabrycky, D., & Tremaine, S. 2007, ApJ, 669, 1298
Gaudi, B. S., & Winn, J. N. 2007, ApJ, 655, 550
Hébrard, G., et al. 2008, A&A, 488, 763
Hirano, T., Suto, Y., Taruya, A., Narita, N., Sato, B., Johnson, J. A., & Winn, J. N. 2010, ApJ, 709, 458
Lin, D. N. C., Bodenheimer, P., & Richardson, D. C. 1996, Nature, 380, 606
Lubow, S. H., & Ida, S. 2010, in Exoplanets, ed. S. Seager (Tucson: University Arizona Press) (arXiv:1004.4137)
Matsumura, S., Peale, S. J., & Rasio, F. A. 2010, ApJ, 725, 1995
McLaughlin, D. B. 1924, ApJ, 60, 22
Nagasawa, M., Ida, S., & Bessho, T. 2008, ApJ, 678, 498
Narita, N., et al. 2007, PASJ, 59, 763
Narita, N., et al. 2009a, PASJ, 61, 991
Narita, N., Sato, B., Hirano, T., & Tamura, M. 2009b, PASJ, 61, L35
Narita, N., Sato, B., Hirano, T., Winn, J. N., Aoki, W., & Tamura, M. 2010, PASJ, 62, 653
Narita, N., Sato, B., Ohshima, O., & Winn, J. N. 2008, PASJ, 60, L1

Ohta, Y., Taruya, A., & Suto Y. 2005, ApJ, 622, 1118
Ohta, Y., Taruya, A., & Suto Y. 2009, ApJ, 690, 1
Pont, F., et al. 2010, MNRAS, 402, L1
Queloz, D., et al. 2010, A&A, 517, L1
Queloz, D., Eggenberger, A., Mayor, M., Perrier, C., Beuzit, J. L., Naef, D., Sivan, J. P., & Udry, S. 2000, A&A, 359, L13
Rossiter, R. A. 1924, ApJ, 60, 15
Sato, B., Kambe, E., Takeda, Y., Izumiura, H., & Ando, H. 2002, PASJ, 54, 873
Schlaufman, K. C. 2010, ApJ, 719, 602
Shporer, A., Mazeh, T., Pont, F., Winn, J. N., Holman, M. J., Latham, D. W., & Esquerdo, G. A. 2009, ApJ, 694, 1559
Triaud, A. H. M. J., et al. 2010, A&A, 524, A25
Winn, J. N., et al. 2005, ApJ, 631, 1215
Winn, J. N., et al. 2009a, ApJ, 700, 302
Winn, J. N., et al. 2010b, ApJ, 723, L223
Winn, J. N., Fabrycky, D., Albrecht, S., & Johnson, J. A. 2010a, ApJ, 718, L145
Winn, J. N., Johnson, J. A., Albrecht, S., Marcy, G. W., Crossfield, I. J., & Holman, M. J. 2009b, ApJ, 703, L99
Wu, Y., Murray, N. W., & Ramsahai, J. M. 2007, ApJ, 670, 820